Chapter 1

Introduction

In this chapter, we present all the fundamental information related to the study conducted and reported in this thesis. We will start with the discovery of magnets, which marks the beginning of the field of magnetism and modern condensed matter physics.

1.1 Magnetism

Magnetic materials and spin systems have been the all-time favourite subject of scientists. These materials show intriguing properties and have been shown to be of much use to humankind. There have been various scientific studies conducted to learn and predict the behaviours of magnetic materials over the centuries. One of the early discoveries, dating to 600 BC—the Greeks discovered rock formations called "lodestones" or magnetite, which turned out to be naturally magnetised. The Greek word magnetis means the stone from Magnesia (Manisa in modern-day Turkey). The place where it was discovered was Magnesia, and hence, the name "magnets" became popular. The first ever compasses were made with suspended pieces of lodestones so that they could rotate freely. The earliest surviving writings about magnets and their properties are from Anatolia, India and China, and they are 2500 years old. By the 11^{th} century AD, the Chinese learned how to make

permanent magnets from iron by heating and quenching iron in the Earth's magnetic field. This led to the discovery of the navigational compass [2]. The discovery of the navigational compass paved the path to new trade routes and directed the course of history.

Many scientists embarked on their journey to explain this mysterious yet intriguing force of nature. An Englishman named William Gilberts (1540-1603) was the first to scientifically investigate the properties of magnets. He discovered that Earth itself has a tiny magnetic field. Carl Friedrich Gauss (1777-1855) studied the Earth's magnetism. He made a magnetometer to measure the direction and strength of the magnetic field. In 1820, Hans Christian Orsted discovered that a compass needle deflects when placed near a current carrier. Andre-Marie Ampere, in the same year, showed that iron gets magnetised if kept inside a solenoidal conducting current. Using this idea, William Sturgeon in 1824 made the electromagnet. Later, electromagnets were found to be applicable in various industries and households. The magnetic ore separator is a key example. At the same time period, Michael Faraday performed a series of experiments on electromagnetic induction, which laid the foundation of modern-day electromagnetism. Later, Maxwell studied electromagnetism theoretically, and showed that the same force field appears as electricity and magnetic. Pierre Curie demonstrated that for materials like iron, for temperatures greater than a specific value magnetism is lost suddenly. Below the Curie temperature, the materials retain their magnetism, either ferro/ferri magnetism. Above it, they become paramagnetic [3]. This discovery led to the modern condensed matter notion of spins as tiny magnets causing various magnetic effects. Various scientists hypothesised several mechanisms to explain this phase transition. Currently accepted models are based on the work by Ernest Ising(Ising model) and Werner Heisenberg(Heisenberg model) in 20^{th} century. We will discuss about their work in detail in the section 1.4. Our current knowledge of magnetism is mainly described the quantum mechanical version of two models, considering spins as quantum operators. The field of magnetism and condensed matter has come a long

way since the early encounter of magnetism. Researchers are currently focused on the study of topological materials and emergent phenomena. The rising interest in topological materials started with the discovery of the quantum Hall state [4]. Detailed discussion about topological materials and terminologies can be found in the section 1.5.

In the quantum mechanical examination of condensed matter physics, our consideration consistently involves numerous interacting spins arranged in an orderly lattice. Therefore, it becomes crucial for us to comprehend spins, spin interactions, and lattices.

In preceding sections, we explored the fundamental building blocks responsible for the magnetic properties of matter–namely, the magnetic moments. According to contemporary understanding, the origin of magnetism can be attributed to the orbital motion of electrons and the spin of the electrons. The movement of electrons in their orbits resembles an electric current, resulting in the atom possessing an orbital magnetic moment. Simultaneously, the intrinsic spin of the electron contributes a magnetic moment component known as the intrinsic magnetic moment. When examining an atom with both orbital and spin magnetic moments, the quantum mechanical sum of the two is always taken into account.

1.2 Spin

Spin constitutes a purely quantum mechanical concept and represents an intrinsic property [5]. The vector atom model, proposing the theoretical framework for spin, was introduced by Goudsmit and Uhlenbeck. Subsequent experimental validation came through the work of Stern and Gerlach in the renowned "Stern-Gerlach experiment." In this experiment, a silver atom beam generated by an oven traversed a nonuniform magnetic field, resulting in the observation of two spots on the screen. The symmetry, in the absence of fields, yields no deflection. The two spots correspond to the two states of a spin$1/2$ particle.

The observed phenomenon is elucidated by considering electron's spin, which gives rise to the magnetic moment within an atom **S**, i.e., $\mu \propto \mathbf{S}$. The energy associated with the magnetic moment and the magnetic field is expressed as:

$$E = -\vec{\mu}.\vec{B}. \tag{1.1}$$

A nonuniform magnetic field ($\mathbf{B} \equiv \vec{B}$) exerts a force on the silver atoms, with consideration given only to the z-component due to the atom's substantial mass. The force resulting from the z-component of the magnetic field, which acts on the atom, is expressed as:

$$F_z = \frac{\partial}{\partial z}(\vec{\mu}.\vec{B}) \simeq \mu_z \frac{\partial B_z}{\partial z}. \tag{1.2}$$

The direction of the force on the atom is contingent upon the value of the z-component of the magnetic moment (μ_z). If $\mu_z > 0$, a downward force is exerted on the atom; conversely, if $\mu_z < 0$, an upward force is applied. Consequently, the beam of silver atoms is divided based on the μ_z value, revealing that the silver atoms strike the plate only in two regions symmetrically positioned around the point of no deflection.

The silver beam's variation is characterised by only two components, implying that the magnetic moment vector of silver atoms must possess only two orientations. The proportional relationship between magnetic moment and spin implies that the z-component of spin also has two orientations. This experimental outcome corroborates the theoretical proposition of spins.

From a quantum mechanical point of view, spins are considered to be mathematical operators. A spin$1/2$ operator is an operator of dimension 2×2. The quantum state of a spin resided in the Hilbert space of dimension 2. However, the dimensionality changes when more than one spin interacts with the other.

1.2.1 Collection of interacting spins

Now we are going to consider the scenario where the system has two interacting electrons. Each of the electrons is represented by a spin-half quantum operator. And they follow certain rules. Consider two electrons with their orbital degrees of freedom suppressed, leaving only their spin degrees of freedom. The total spin operator for this system of two electrons can be expressed as:

$$\mathbf{S} = \mathbf{S_1} \otimes \mathbb{1} + \mathbb{1} \otimes \mathbf{S_2}, \tag{1.3}$$

Here, $\mathbb{1}$ denotes the identity operator with dimensions 2×2, and it is positioned in the spin space of electron 2 (or 1) in the first (or second) term. The individual spins belong to a Hilbert space of two dimensions each, and the entire system of two electrons is described by a Hilbert space of $2 \otimes 2$ (i.e., 4 dimensions).

The commutation relations of spin operators, both at the same site and different sites, are provided as follows:

$$[S_{1x}, S_{1y}] = \mathrm{i}\hbar S_{1z},\ [S_{2x}, S_{2y}] = \mathrm{i}\hbar S_{2z}, \quad [S_{1p}, S_{2q}] = 0. \tag{1.4}$$

The commutation relations for the spin operators are given above. Note that for the last commutation relation, it holds no matter what component p or q may represent. Here $\mathbf{S^2} = (\mathbf{S_1} + \mathbf{S_2})^\mathbf{2}$, $S_z = S_{1z} + S_{2z}$, S_{1z}, and S_{2z} have eigenvalues $s(s+1)\hbar^2$, $m\hbar$, $m_1\hbar$, and $m_2\hbar$, respectively. The ket vectors corresponding to the spin state of two electrons, expressed in terms of the eigenkets of $\mathbf{S^2}$ and S_z, can be written as $|s = 1, m = \pm 1, 0\rangle$ and $|s = 0, m = 0\rangle$, where $s = 1$ represents the spin-triplet ($2s + 1 = 3$) state, and $s = 0$ represents the spin-singlet ($2s + 1 = 1$) state. For the spin-triplet ($s = 1$) state, there are three basis vectors $|s = 1, m = 1\rangle$, $|s = 1, m = 0\rangle$, and $|s = 1, m = -1\rangle$, while for spin-singlet ($s = 0$) state, there is one basis vector, namely $|s = 0, m = 0\rangle$.

Now, for instance, consider the interaction between the two spins to follow:

$$\hat{H} = J_{12}\mathbf{S_1}.\mathbf{S_2}. \tag{1.5}$$

where J_{12} represents the interaction strength. The value of $\hat{H}$ is contingent on $\mathbf{S_1}.\mathbf{S_2}$. The calculation of $\mathbf{S_1}.\mathbf{S_2}$ for the singlet and triplet states involves the expression $\mathbf{S_1}.\mathbf{S_2} = (\mathbf{S}^2 - \mathbf{S_1}^2 - \mathbf{S_2}^2)/2$, yielding the values $-\frac{3J_{12}\hbar^2}{4}$ for the singlet state and $\frac{J_{12}\hbar^2}{4}$ for the triplet state. Note that for spin $1/2$ $s_1 = s_2 = 1/2$. If $J_{12} > 0$, the singlet state has lower energy, indicating a ferromagnetic state. Conversely, if $J_{12} < 0$, the triplet state has the minimum energy, signifying an antiferromagnetic state.

In condensed matter physics, we employ theoretical models to get insight into various physical phenomena in materials. The typical model consists of a lattice of spins and interaction terms between spins at each lattice site. Various lattice geometries are very well understood. In all our discussions, we use either a triangular lattice or a square lattice, and we have used some sophisticated boundary conditions. We cannot talk about lattice and interacting quantum systems without talking about the underlying boundary conditions. In the subsequent sections, we will explore boundary conditions and typical models of $N(N > 2)$ interacting spins.

1.3 Boundary conditions

Our aim is to model physical systems as accurately as possible. The lattices we consider for modelling depend on the kind of physical model we are interested in. Depending on the dimension of the problem, we have several lattices to choose from.

1.3.1 One dimension

In one-dimensional problems, we consider a chain of spin arrangements (Fig. 1.1.(B)). Here, each lattice site is at a constant lattice distance away from the nearest neighbouring site. The lattice sites at the extreme ends are considered to be the "boundary" sites. In this arrangement, there are two boundary sites. All of the interactions we mentioned earlier occurred between two neighbouring sites. A site interacts with the site immediately to its right. However, considering the rightmost site, it does not have a neighbour on its right side with which to interact. This is where the boundary condition comes into play. Depending on the kind of problem at hand, we can use various boundary conditions here.

1. Open Boundary (Fig. 1.1a). The rightmost site has only one interacting term with the site on its immediate left. This keeps the chain "Open". Hence the name open boundary. This is preferred when we model small-scale systems. For example, when we study nanoscale structures.

2. Closed/Periodic boundary (Fig. 1.1b).

   Here, the rightmost site also interacts with the leftmost site, making a closed loop(Fig. 1.1.(B)). Hence, the name closed/periodic boundary. This is preferred when we are modelling the system to look for bulk properties.

Apart from these common boundary conditions, we may use other ingenious ways to make boundaries. If the system is embedded within a larger system that has its own properties. Depending on those properties, boundary terms can have a multitude of boundary interaction terms. For example, a ferromagnetic boundary.

1.3.2 Higher dimension

We can extend the idea of these boundary conditions to higher dimensions as well. In higher dimensions, we have many lattice geometries, and so the number of interactions

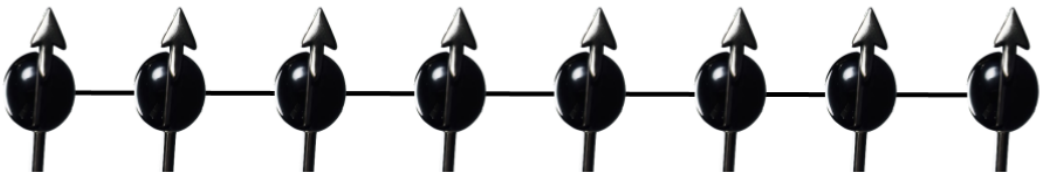

(A)

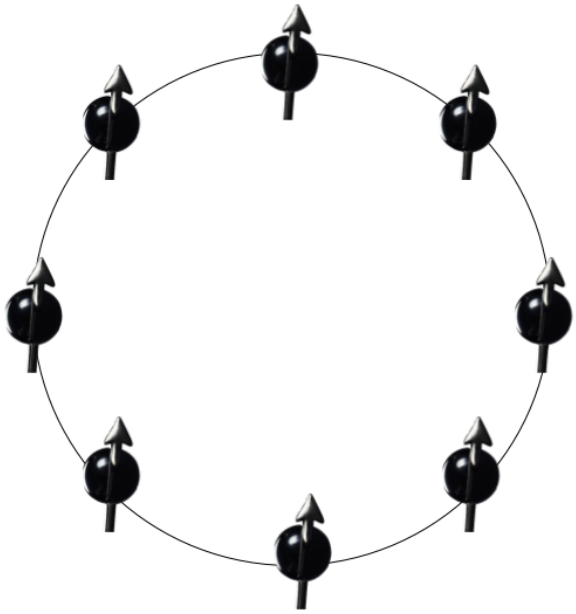

(B)

Fig. 1.1 A) One-dimensional quantum spin chain with open boundary. A solid line connecting neighbouring spins indicates interaction. B) One-dimensional quantum spin chain with closed/periodic boundary. The first spin interacts with the last spin to form a closed loop.

varies between neighbouring sites. But the idea remains the same. For example, in a two-dimensional square lattice, considering open boundary conditions, the sites at the four corners have two fewer interaction terms. The rest of the boundary sites, apart from the cornering ones, have one fewer interaction term. The periodic boundary condition can be applied either along the horizontal lattice direction, along the vertical lattice direction or along both directions, depending on the problem.

There are many more choices for boundaries in higher dimensions. We limit our discussions to this much. In the next chapter, we can see an example of a periodic boundary condition applied to a circular supercell formed in a triangular lattice. In Chapter 5, we use a classical ferromagnetic boundary condition to model a skyrmion embedded in a ferromagnet.

Let us now explore some well-known spin models commonly used to describe spin systems.

1.4 Spin models

1.4.1 Ising model

The Ising model, a classical mathematical framework within statistical mechanics, was proposed by the German physicist Ernst Ising in 1925. Ising formulated the Ising model as his doctoral thesis under the guidance of Wilhelm Lenz at the University of Hamburg. Ising introduced this model to investigate the behaviour of magnetic moments in a crystalline lattice, with a primary focus on gaining insights into phase transitions. The original purpose of the model was to explore the magnetic properties of ferromagnetic materials, specifically aiming to understand the emergence of ferromagnetism in a crystalline lattice. Initially, Ising developed a one-dimensional version of the model, considering a linear chain of spins with binary values (up or down) [6]. Ising showed that the one-dimensional model

has no phase transition. Following a series of approximate calculations, Ising seemingly indicated that his model could not demonstrate a phase transition in both two and three dimensions. However, later investigations revealed that this conclusion was inaccurate [7, 8].

The Hamiltonian considered by Ising follows: For system of N spins $1/2$ arranged in a one-dimensional chain.

$$H = -J\sum_{ij} S_i^z S_j^z - \mu B \sum_{i=1}^{N} S_i^z \tag{1.6}$$

Here, the first term is the nearest neighbour exchange term, J is the coupling constant, and the second term is the Zeeman term or the applied magnetic field. Depending on the magnitude of the coupling constant, J, the ground state of the Ising model can vary. If $J < 0$, the ground state will follow an alternating up-down spin arrangement, resulting in an antiferromagnetic ordering. Alternatively, when $J > 0$, then the system prefers an all-spin-parallel configuration, leading to a ferromagnetic ground state. The parameter B can govern the phase transition between these phases even in the absence of thermal activation. More about phase transitions can be found in section 1.6

1.4.2 Heisenberg model

The Heisenberg model can be thought of as an extension of the Ising model. Here, all three spin components are considered while writing the spin-spin interaction.

Let's consider a lattice comprising N sites, where N approaches infinity. At each lattice site i, a spin vector $\vec{\mathbf{S}}_\mathbf{i}$ is positioned. The interaction between spins is characterized by $\vec{\mathbf{S}}_\mathbf{i} \cdot \vec{\mathbf{S}}_\mathbf{j}$. Considering all possible pairs of spin-spin interactions, the Hamiltonian is expressed as:

$$H = \sum_{i \neq j} J_{ij} \vec{\mathbf{S}}_\mathbf{i} \cdot \vec{\mathbf{S}}_\mathbf{j}, \tag{1.7}$$

Here, the indices i and j iterate from site 1 to N on the lattice. The coefficient J_{ij} denotes exchange constants or interaction strength and possesses symmetry, i.e., $J_{ij} = J_{ji}$. The strength of interaction diminishes with an increasing distance between indices i and j. The value of J_{ij} can take either positive or negative values. A negative J_{ij} is favoured when spins are aligned in parallel, indicating ferromagnetic behaviour (Fig. 1.2 (left)) found in **Co and Fe**. Conversely, a positive J_{ij} is favoured in the case of an antiparallel alignment of spins, indicating antiferromagnetic behaviour (Fig. 1.2 (right)) as seen in **Fe/Mn and NiO**. The exchange interaction always results in a collinear arrangement of spins. This is due to the inversion symmetry-preserving nature of the interaction. A broken inversion symmetry is the key to achieving non-collinearity and various quantum phases like helical, Skyrmion and vortex.

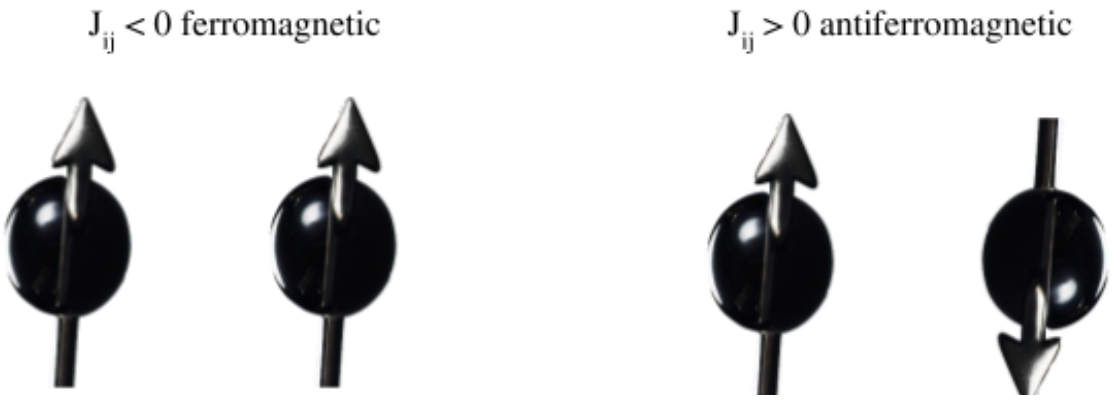

Fig. 1.2 Ferromagnetic exchange interaction (left). Antiferromagnetic exchange interaction (right).

The commutation relations for spin components at the same site are given by:

$$[S_j^\alpha, S_j^\beta] = i\varepsilon_{\alpha\beta\gamma} S_j^\gamma \qquad (\alpha, \beta, \gamma = x, y, z), \tag{1.8}$$

where $\varepsilon_{\alpha\beta\gamma}$ is the Levi–Civita symbol. Its value is $+1(-1)$ if α, β, γ are in cyclic (non-cyclic) order and 0 when at least any two variables (α, β, γ) are the same. However, spins at different sites commute with each other, i.e., $[S_i^\alpha, S_j^\beta] = 0$.

1.4.3 Dzyaloshinskii–Moriya interaction term

The Dzyaloshinskii–Moriya interaction (DMI)[9, 10] is a form of antisymmetric interaction that compels neighbouring atomic spins to orient themselves perpendicular to one another. While the Heisenberg interaction typically favours parallel (ferromagnetic) or antiparallel (antiferromagnetic) states between two spins, the DMI introduces a rotational influence, causing spins to rotate either clockwise or counter clockwise. The presence of DMI necessitates a broken inversion symmetry and significant spin–orbit coupling (SOC). This interaction serves as a crucial element in the manifestation of noncollinear magnetism and chiral magnetism, giving rise to chiral domain walls and magnetic skyrmions. Quantitatively, it is a term within the Hamiltonian expressed as:

$$H^{(DM)} = \mathbf{D_{ij}}.(\mathbf{S_i} \times \mathbf{S_j}). \tag{1.9}$$

When the total Hamiltonian is considered, it is summed over the lattice sites in the same fashion as Heisenberg's term. $\mathbf{D_{ij}}$ are Dzyaloshinkii–Moriya vectors.

The direction of these vectors depends on the unit vector from site i to site j. In Fig. 1.3, two spins $\mathbf{S_i}$ and $\mathbf{S_j}$ interact with each other through the diamagnetic atom represented by a red circle. $\mathbf{d}$ is the vector from the centre of the line joining $\mathbf{S_i}$ and $\mathbf{S_i}$ and the centre of the diamagnetic atom. $\mathbf{a_{ij}}$ is the unit vector from i to j, which makes $\mathbf{D_{ij}} = \mathbf{d} \times \mathbf{a_{ij}}$. Usually, the strength of interaction falls steeply with the increasing distance between neighbouring sites. Because of this, for most of the models, only nearest neighbouring interactions are adequate to provide insight.

However, for some instances we may consider second and higher order neighbouring interactions, to account for some exotic behaviours shown by magnetic materials. For instance, consider the Heisenberg term. Suppose the nearest neighbours follow $J_{ij} < 0$ and the next nearest neighbours follow $J_{ij} > 0$. This will lead to frustration in the system when choosing whether to align parallelly or antiparallelly, leading to exotic states like spin-

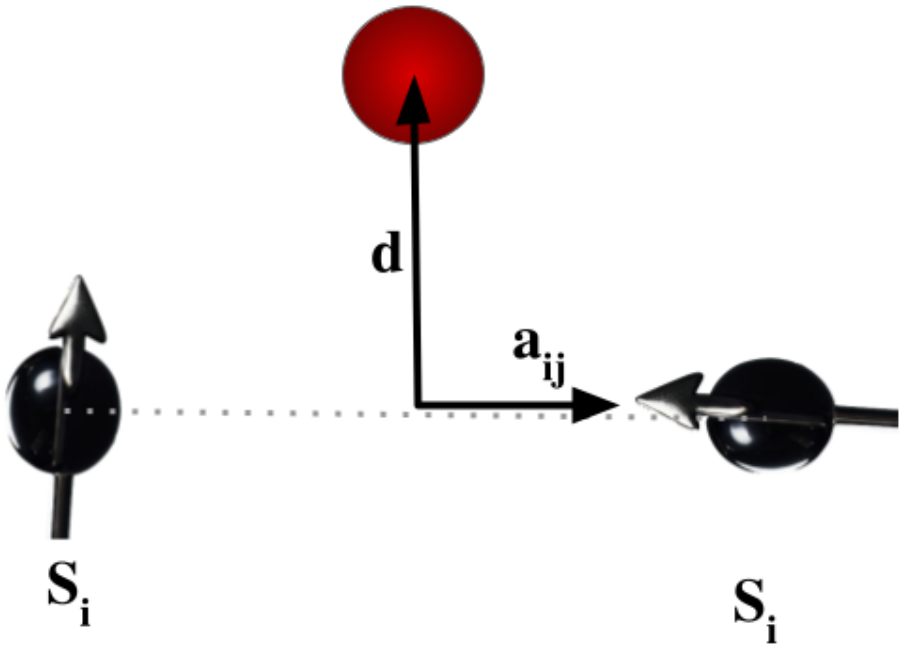

Fig. 1.3 Schematic representation of how to find the direction of the DMI vector. Here, two spins at i and j interact with each other through the SOC excited orbit of the diamagnetic atom in red colour.

glasses and liquids. We will not look into the details of these. However, we will discuss about how these interactions supplement the formation of skyrmions in the upcoming chapters.

We will now briefly discuss another important aspect of this thesis: topology and topological materials.

1.5 Topological materials

When a two-dimensional electron gas is applied with an external field, the quantum Hall state demonstrates a Hall conductivity that is quantised to an integer ratio. The cause for this observation is linked to a topological invariance [11]. This observation, now known as the quantum Hall effect, opened the path to the then-uncharted territory of topology in matter. Next came the topological insulators. These materials are insulators in their bulk

but show metallic nature on their boundary/surface owing to some topological ordering [12]. If we look at these two examples of topological states closely, we can identify some key characteristics peculiar to topological states, such as topological invariance and topological ordering. Before we introduce any more topological states, let us try to have a general understanding of what we mean by topology in condensed matter physics and what its distinguishing characteristics are.

Consider the case of the quantum Hall effect, we mentioned a quantised integer ratio, which is followed by the Hall conductance. This is a characteristic feature of a topological state. To be precise, a topological state tends to have some characteristic feature that tends to be an invariant (constant) across local perturbations. That is, we can associate a parameter with a topological state, which will remain an invariant with respect to local perturbations that do not close the bulk energy gap. Topological ordering is an umbrella term that is used to describe the emergent properties associated with the topology of the state.

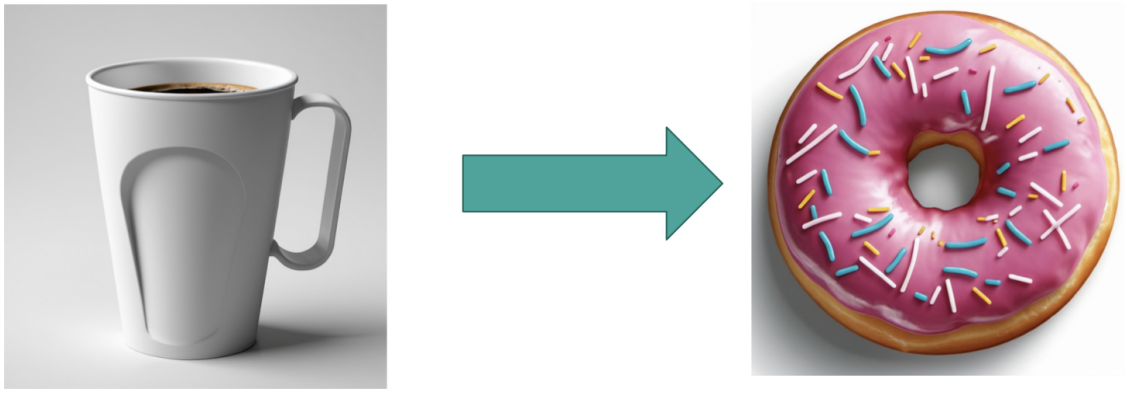

Fig. 1.4 Cup with a handle has only one hole, which is the loop forming the handle. A doughnut also has only one hole at the centre. (Figures generated using generative AI DALL.E by OpenAI [1])

The field of topology deals with the properties of objects that are invariant under smooth deformations. Topology studies shapes that can morph into each other without tearing or glueing, like a doughnut smoothly twisting into a coffee cup Fig. 1.4. It's all

about properties that stay the same even when the shape bends and stretches, like the number of holes, which remains unchanged in our doughnut coffee cup transformation. By smooth deformation, we meant that we do not need to introduce new holes or remove existing ones in order to smoothly transform a doughnut into a coffee cup. That is, we do not need to 'cut' the doughnut in order to transform it into a coffee cup. But if we need to transform a doughnut into a pretzel, we need to cut the doughnut to introduce more holes. So we can say that the number of holes remains invariant for topologically identical objects. For a topological insulator, the deformation is applied to the state. We can also identify an invariant that remains constant, similar to the number of holes, when a smooth deformation is applied. For a topological insulator, its surface shows metallic behaviour unless a topological invariant (Chern number) remains unchanged. The surface becoming insulating is always associated with a change in the value of the Chern number. Another term that we will encounter very often in the case of the topological materials is the topological protection. Topological protection is used to describe the resilience of certain properties of a material that are deeply ingrained in its internal structure, such that local perturbations like impurities cannot easily destroy or alter them. This can be considered as an alternate definition of a topological state.

The realm of topological materials is vast. Topological materials and states like topological insulators (TI) [13, 14], topological crystalline insulators (TCI) [15, 16], topological semimetals [17, 18], topological Weyl and Dirac semimetals [19], chiral topological superconductors [20], etc. are being studied extensively. Recent applications of topological quantum chemistry to discovery of high-throughput materials has concluded that most of the solid state,stoichiometric, and nonmagnetic materials show topological nature at the Fermi level. 85% of stoichiometric materials discovered show energetically isolated topological bands, and most of the energetically isolated bands show a topology of a TI or a TCI [21]. There are several theoretical models that predict topological states.

Electrons are fermionic, and there is theoretical and experimental evidence of bosonic topological effects aided by magnons. As a bosonic analogue of the topological insulator, topological magnon insulator is examined. It is probed experimentally [22, 23] and studied theoretically [24, 25] in a honeycomb lattice with DMI [9, 10].

Since magnons are charge-free particles, experimental probing of the topological magnon insulator through the Hall effect is not feasible. There have been alternate attempts at probing the topological magnon insulator through thermal Hall effect measurements, which is theoretically suggested [26, 27] and experimentally realised [28].

The research on topological states is interesting because of their anticipated uses. One of the most discussed applications is in topological quantum computing. The topological insulator–superconductor interphase is anticipated to generate new emergent particles that may include the formation of zero-energy Majorana fermions [29, 30]. The observation of Majorana fermions brings the efforts to produce a topological quantum computer one step closer to the goal. The Majorana fermions, due to their peculiar quantum numbers, obey non-Abelian quantum statistics. This helps to protect the quantum computers from errors [31].

The world of technology is anticipating great feats from topological materials, a class of substances with unique properties that defy conventional physics. These materials hold immense promise for revolutionising fields like:

1. Quantum computing: Topological materials could be the key to building robust and fault-tolerant quantum computers [31].

2. Spintronics: The idea to harness the spin of electrons instead of their charge for data storage and processing. Topological materials offer exceptional advantages for spintronics devices, including lower power consumption, faster operation [32, 33].

Topological materials possess unique electronic or magnetic properties that are "topologically protected," meaning they are robust and resilient to disturbances. This opens up a treasure trove of possibilities for engineers and scientists, paving the way for:

1. Ultra-efficient electronics: Topological insulators, a specific type of topological material, can conduct electricity on their surfaces while remaining insulating in their bulk. This allows for lossless transmission of electrons, leading to devices that consume significantly less power than current technologies [34, 35, 36].

2. High precision sensors: The unique properties of topological materials can be harnessed to create highly sensitive optic sensors [37].

   Noncollinear magnetism and related discoveries are subsequent developments to the conventional magnetic behaviours we discussed earlier. Many of the topological orders are associated with noncollinear magnetism [38, 39]. We will discuss about them in detail in the next section.

1.5.1 Noncollinear magnetism

In case of conventional magnetic materials, the magnetic moments within the materials neatly align either parallel or antiparallel to each other. Imagine a bunch of tiny bar magnets, all lined up like soldiers in a parade. This is pretty much how magnetism works in conventional materials. The magnetic moments neatly arrange themselves either parallel (shoulder to shoulder) or antiparallel to their neighbours. The underlying interactions between these magnetic moments, governed by factors like temperature and external fields, determine the material's magnetic phases.

Many materials exhibit magnetic unit cells that deviate from the simple distinctions of being ferromagnetic or antiferromagnetic. Instead, they showcase a more intricate magnetic structure where the orientation of magnetic moments varies among different

atoms within the unit cell. These magnetic structures are termed noncollinear and can arise from various factors. Magnetic frustration, wherein the preferred alignment of magnetic moments at different atoms conflicts with the system's geometry, is one possible cause. Another contributing factor could be SOC.

In case of non collinear magnetism, magnetic moments can twist and turn, forming a swirling, corkscrew-like arrangement, helices, spirals and vortexes instead of lining up neatly. The constituent magnetic moments, apart from collinear arrangements, can also align in a twisted fashion. This concept is against our intuitive understanding of magnets. Even the tiniest of magnets has two poles. Unlike poles attract to each other, and like poles repel from each other. This effectively leads to a collinear (either parallel or antiparallel) alignment of the magnets. Although that is still true for individual magnets, in noncollinear magnetism, it is not just single magnets, but a coordinated dynamic arrangement of many. Within the swirl, neighbouring moments can be "north-south" pairs, but the overall pattern twists and turns, defying our classical intuition. The non collinear spin formations in magnetic material are responsible for chiral magnetism. The spin helices, spirals and vortices can have handedness(chirality).

1.5.2 Chirality

Chirality pertains to the condition where an object and its reflected image cannot align through spatial rotation and translation; in other words, all mirror symmetries are broken or absent in the object, even with unrestricted spatial rotation and translation. A well-known illustration of chirality is found in our hands: the left hand cannot be perfectly superimposed onto its mirror image, the right hand, despite allowing for spatial rotation and translation. Furthermore, chirality in stable states maintains time-reversal symmetry, indicating that left-handed chiral objects remain left-handed even under a time-reversal symmetry operation.

When discussing magnetic chirality, we are referring to chirality observed in spin-ordered states or spin textures at the atomic or mesoscopic scale. In this thesis, our main focus is on topological quasi-particles called skyrmions. Skyrmions are stable chiral magnetic structures formed within magnetic materials. Like any other topological states, skyrmions also possess fascinating properties which have captivated the minds of contemporary physicists.

An important quantity that helps characterise the chiral nature of the spin structure is the **vector chirality** or the **scalar spin chirality**, depending on the situation.

The **vector chirality** between two neighbouring spins, $\mathbf{S}_i$ and $\mathbf{S}_j$, is defined as

$$\kappa_{ij} = \mathbf{S}_i \times \mathbf{S}_j. \tag{1.10}$$

Where the cross product captures the sense (right-handed or left-handed) of rotation between the two spins. In systems with continuous spin textures, such as helical magnets, vector chirality acts as an order parameter that distinguishes different chiral states.

In more complex magnetic structures like skyrmions, it is often more appropriate to consider the **scalar spin chirality**. For three neighbouring spins, $\mathbf{S}_i$, $\mathbf{S}_j$, and $\mathbf{S}_k$, the scalar chirality is defined as

$$\chi_{ijk} = \mathbf{S}_i \cdot (\mathbf{S}_j \times \mathbf{S}_k). \tag{1.11}$$

Where the scalar quantity measures the solid angle formed by the three spins. A nonzero average scalar chirality signals the presence of nontrivial topological textures such as magnetic skyrmions. It is also responsible for emergent electromagnetic effects that influence the motion of electrons inside the material.

Thus, in the context of magnetic chirality, both vector chirality and scalar spin chirality serve as important order parameters that describe and govern the underlying chiral magnetic states, particularly in systems exhibiting topological features like skyrmions.

1.5.3 Magnetic skyrmions

In field theory, a skyrmion represents a topologically stable configuration emerging from a class of nonlinear sigma models. First introduced by Tony Skyrme, this idea centres around a topological soliton whose stability is ensured by the spatial topology of the field, originally formulated to model nucleons [40]. Although skyrmions are now understood not to be fundamental particles, their quasi-particle behaviour remains a topic of intense interest, especially within condensed matter physics. These vortex-like entities have been experimentally realized in a range of systems, including Bose–Einstein condensates [41], liquid crystals [42], quantum Hall regimes, acoustic media [43], and photonic environments [44].

This thesis focuses on magnetic skyrmions—two-dimensional (2D) topological entities defined by localized spin configurations that transition smoothly from the centre to the periphery while maintaining a consistent helicity. As an illustration, Fig. 1.5 depicts two distinct types of these spin variations.

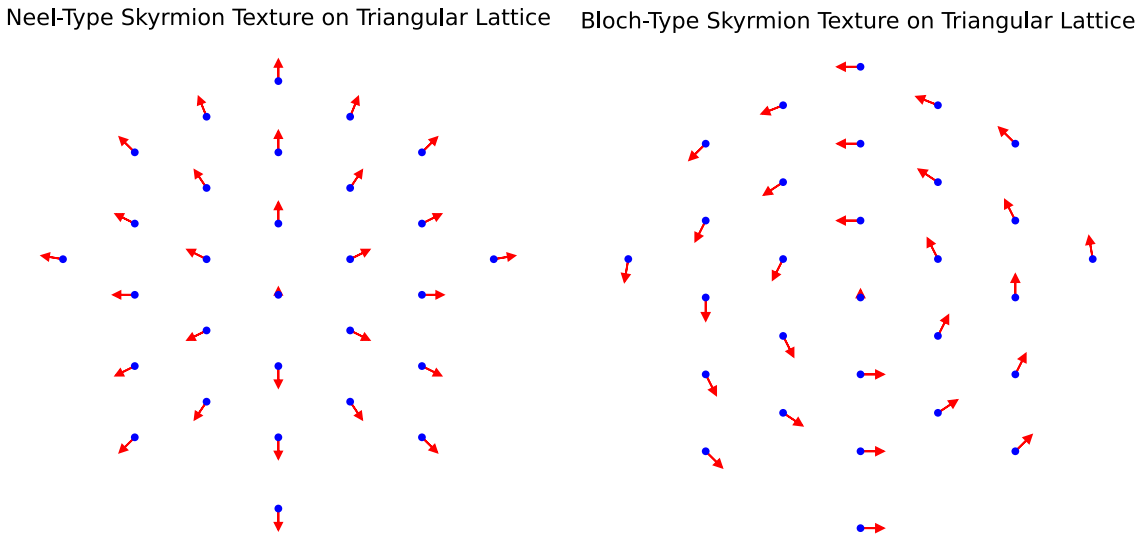

Fig. 1.5 Neel-type skyrmion (left) and Bloch-type skyrmion (right)

In the case of a Neel-type skyrmion, the spins tend to rotate within radial planes as they move from the core towards the outer edge. This means the direction of the spin vectors

changes in accordance with the radial distance from the centre, with the spins gradually rotating as they move outward. The spin vectors undergo a continuous variation, with their orientation influenced by the core's position, resulting in a smooth and uniform transition from the centre to the periphery. In contrast, rotating spins along the tangential planes (perpendicular to the radial directions) are the peculiarity of the Bloch-type skyrmion. As the spins move away from the core, they do not align with the radial direction but instead rotate within planes that are tangential to the radial lines. This leads to a rotation pattern in which the spins change orientation in a direction that is perpendicular to the outward radial movement, creating a rotation pattern distinct from that of the Neel-type skyrmion.

First observed experimentally in a chiral magnet in 2009 [45], the Dzyaloshinskii–Moriya interaction (DMI), also known as the antisymmetric exchange interaction, is a key mechanism for stabilizing skyrmions in materials with non-centrosymmetric crystal structures [46] and at interfaces where inversion symmetry is inherently broken [47]. However, skyrmions have also been found in certain centrosymmetric systems, demonstrating exceptions to this general trend [48, 49, 50, 51]. These interactions will be examined in greater detail in the sections that follow. Unlike other magnetic nanostructures such as chiral domain walls—investigated for their potential use in energy-efficient spintronic technologies—skyrmions exhibit robust stability due to their nontrivial topology. Additionally, their ability to move under low-energy current makes them promising candidates for practical device integration [52, 53, 54, 55, 56].

Currently, magnetic skyrmions are gaining prominence as promising candidates for applications involving data storage owing to their small sizes, stability, and tunable responses to external perturbations. Over a decade of intensive research has unveiled promising architectures such as ferromagnet/heavy metal (FM/HM) interfaces, ferrimagnet/HM interfaces, and synthetic antiferromagnets (SAFs). Additionally, the dynamics of current-driven skyrmions have expanded the application possibilities of these structures. The rapid

development in this field has prompted numerous excellent reviews focusing on their topological properties, the diverse hosting crystals and multilayers, and progress in their applications. Skyrmions have been observed in numerous hosting materials [57]. Owing to the nanoscale structure of the skyrmion, the quantum effects prevail. The quest for a quantum mechanical description of the quasiparticle is a primary objective in this thesis. The focus is squarely on addressing this challenge, and the remainder of this chapter will delve into the foundational principles and tools essential for tackling this task.

So far, we have discussed various phases observed in magnetic systems. Let us now see how phase transitions are understood in this framework. This discussion holds significant importance in laying the foundation for the chapters to follow.

1.6 Phase transition

In chemistry and thermodynamics, a phase transition is when a substance changes from one state to another, like from a solid to a liquid or a gas. This often happens when you change the temperature or pressure. For example, when you heat a liquid to its boiling point, it can quickly turn into a gas. The specific conditions where this change occurs are called the phase transition point.

During a phase transition, some of the properties associated with the materials change. Sometimes the change is continuous, and sometimes it is discontinuous or abrupt. Phase transitions occur at specific points in a system's parameter space where a slight adjustment in the control parameter leads to a significant transformation in its characteristics.

Paul Ehrenfest devised a classification system for phase transitions regarding the thermodynamic free energy behaviour concerning other variables [58]. In this categorisation, phase transitions are identified by the free energy's lowest derivative that experiences discontinuity during the transition. For instance, first-order phase transitions, show a discontinuity in the free energy's first derivative with respect to a particular thermodynamic

variable [59]. Transitions between solid, liquid, and gas states fall into the first-order category due to the abrupt change in density, representing inverse of the free energy's first derivative, which depends on pressure.

In contrast, second-order phase transitions are marked by the continuity of the first derivative of the free energy—typically represented by the order parameter, which remains smooth across the transition. However, a discontinuity appears in the second derivative of the free energy [59]. A classic example is the ferromagnetic transition in elements like iron, where the magnetization gradually emerges as the temperature drops below the Curie point. In this case, although magnetization evolves continuously, the magnetic susceptibility– corresponding to the second derivative of the free energy with respect to the external magnetic field–exhibits a discontinuous shift. According to Ehrenfest's classification, the possibility exists for third, fourth, and higher-order phase transitions in principle. The specific heat of numerous ferromagnetic materials exhibits a sudden change in slope at their Curie points, indicating a third-order transition [60, 61].

Phase transitions are distinctive features in magnetic systems as well. As we discussed in the earlier sections, the transition from ferromagnetic to paramagnetic states, initially observed by Pierre Curie, stands out as a crucial milestone in the evolution of magnetism and condensed matter physics.

In classical phase transitions, the influence of thermal fluctuations plays a key role in disrupting long-range ordering, ultimately facilitating the occurrence of the phase transition. The fundamental cause of the quantum phase transition is quantum fluctuations. In the next section, quantum phase transitions and their features are introduced.

1.6.1 Quantum phase transition

The previously discussed phase transitions happen at non-zero temperatures, where thermal fluctuations disrupt macroscopic order, like the crystal structure during melting. In recent

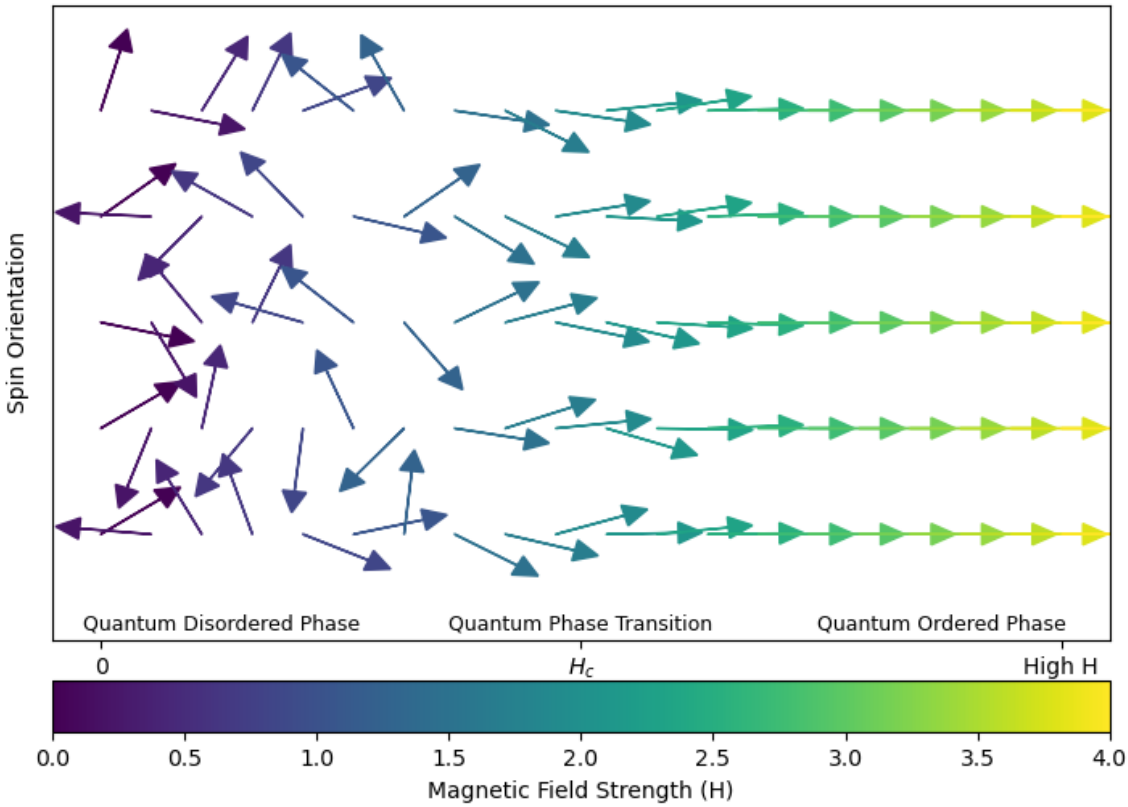

Fig. 1.6 Schematic diagram showing disordered spins going to an ordered arrangement through the application of magnetic field.

times, physicists have become interested in a different type of phase transition occurring at zero temperature. In this case, a non-thermal control parameter, such as pressure, magnetic field, or chemical composition, is adjusted to reach the transition point. At this point, order is disrupted exclusively by quantum fluctuations stemming from the Heisenberg uncertainty principle. A typical example of a quantum phase transition is observed in the transverse field Ising model (TFIM), where the system undergoes a shift from a paramagnetic to ferromagnetic phase. This transition occurs as the externally applied field is gradually increased from a critical value, H_c (1.6), resulting in the total magnetisation of the spin chain smoothly transitioning from a zero to a finite value.

Initially, one might think that investigating these particular points in the phase diagram is a niche area only relevant to experts, given that these transitions occur at a specific value of a control parameter and at the experimentally challenging temperature of absolute zero. However, recent developments in both experimentation and theory have disproven this perception. It has become evident that zero-temperature quantum critical points are crucial for solving previously unanswered questions in various condensed matter systems. Examples of such systems include rare-earth magnetic insulators, heavy-fermion compounds, high-temperature superconductors, and two-dimensional electron gases. The characteristics of quantum fluctuations, which can disrupt long-range order at absolute zero, are significantly different from those of thermal fluctuations that cause conventional phase transitions at finite temperatures. The core idea of quantum phase transitions can be summarised as follows:

Imagine a modification of a parameter (field) occurring at absolute zero temperature. The system's partition function Z is typically expressed as a function of the control parameter and temperature T, denoted as $Z(T)(Z = Tr(e^{-\beta\hat{H}}), \beta = 1/T)$. Quantum phase transitions are linked to the roots or zeros of this partition function. If these roots are real and positive, the associated free energy exhibits non-analytical behaviour, given the inverse relationship between free energy and partition function, $F = -\frac{ln(Z)}{\beta}$. These non-analytical features in the free energy represent quantum phase transitions or equilibrium quantum phase transitions (EQPT).

Dynamical quantum phase transitions (DQPT) are a relatively new concept that we are still trying to understand. DQPT is one of the main areas of our interest because of its novelty and potential for uncovering various entropy features.

1.6.2 Dynamical quantum phase transition

What if we explore the idea of a complex temperature and examine the corresponding partition function and free energy in a quantum system? Michael Fisher pondered on this hypothetical concept and conducted a detailed analysis, identifying the roots of such a partition function with complex temperature.

By considering a complex temperature, denoted as z instead of the conventional temperature T, the partition function becomes $Z(z)$. When the zeros of this partition function coincide with the real axis, it leads to non-analyticities in the corresponding free energy, implying a phase transition but not an Equilibrium Quantum Phase Transition (EQPT).

Let's consider the quantity known as the Loschmidt amplitude, as expressed in Equation 4.2:

$$\mathscr{G}(t) = \langle \psi_0 | e^{-i\hat{H}t} | \psi_0 \rangle. \tag{1.12}$$

This expression is akin to the partition function in thermodynamic equilibrium, where $Z = \mathrm{Tr}(e^{-\beta\hat{H}})$, but with a twist—here, instead of temperature, we have a complex temperature denoted as it. In this context, $\hat{H}$ represents the Hamiltonian, and β is the inverse temperature. The function $\mathscr{G}(t)$ serves a similar role as the partition function of complex temperature considered by Fisher. Consequently, we can define the corresponding free energy, as shown in Equation 4.3:

$$\mathscr{L}(t) = -\lim_{N\to\infty} \frac{1}{N} \ln |\mathscr{G}(t)|^2. \tag{1.13}$$

This is known as the rate function of the return probability, or simply the rate function. The zeros of the Loschmidt amplitude induce non-analyticities in the rate function, serving as the signature of a Dynamical Quantum Phase Transition (DQPT). A schematic of what

to expect at a nonanalytic criticality is shown in Fig. 1.7. The critical point (T_c) is identified by the dashed vertical line on the time axis.

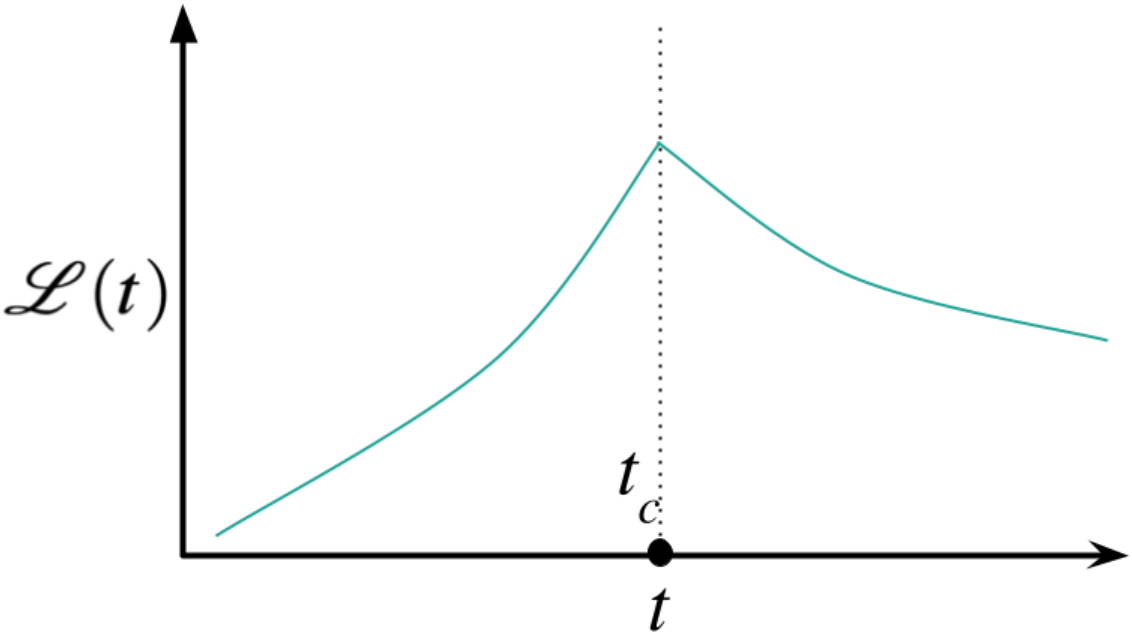

Fig. 1.7 Schematic diagram showing non-analyticity in the rate function.

In the next chapter, we will revisit the concepts underlined in this section. Another emerging field of interest in this decade is quantum thermodynamics. In this thesis, we take some insight from this topic to handle some problems. A more detailed description of the partition function, free energy, and other important quantities is included in the next section.

1.7 Thermodynamics of quantum systems

The field of quantum thermodynamics constitutes an important interdisciplinary area that connects the principles of quantum mechanics with the classical laws of thermodynamics. This subject tries to understand how thermodynamic quantities, such as energy, heat, and entropy, manifest in systems where quantum effects cannot be neglected [62, 63]. Unlike classical thermodynamics, where systems are described by macroscopic parameters,

quantum thermodynamics involves microscopic descriptions based on wavefunctions or density matrices. These systems evolve either unitarily or non-unitarily, depending on their interaction with the environment (explained in upcoming sections).

1.7.1 Basic concepts: quantum states and Observables

State vector, $|\psi\rangle$, describes the state of a system in a Hilbert space $\mathscr{H}$ for pure states, or a density operator ρ for mixed states. The density matrix formulation is particularly significant in quantum thermodynamics, where systems often interact with environments, leading to statistical mixtures rather than pure states.

Observable quantities are represented by Hermitian operators acting on $\mathscr{H}$. An operator A's expectation value of in a given state ρ is given by:

$$\langle A \rangle = \mathrm{Tr}(\rho A).$$

1.7.2 Internal energy and heat

In quantum mechanics, the internal energy of a system is defined as the expectation value of its Hamiltonian:

$$U = \langle H \rangle = \mathrm{Tr}(\rho H),$$

where ρ denotes the density matrix and H is the Hamiltonian of the system. The concept of heat in quantum systems is associated with changes in internal energy that are not attributable to work. For open quantum systems, which are coupled to external environments or reservoirs, the first law of thermodynamics takes the form:

$$dU = \delta Q + \delta W,$$

where δQ and δW represent the infinitesimal heat and work contributions, respectively [64].

1.7.3 Partition function and statistical description

A quantum system, which is thermally equilibrated with a heat bath is described by the canonical ensemble. The corresponding density matrix is given by:

$$\rho = \frac{e^{-\beta H}}{Z}.$$

Where $\beta = 1/(k_B T)$ is the inverse temperature, and the partition function $Z = \mathrm{Tr}(e^{-\beta H})$ contains all the information on the thermodynamic properties of the system. Using the partition function, one can derive thermodynamic quantities, like entropy, Helmholtz free energy, and specific heat [62]. Although the formulation mirrors classical statistical mechanics, additional care must be taken due to the non-commutativity of quantum operators and the potential presence of coherence.

1.7.4 Work in quantum systems

The concept of work in quantum systems is more sophisticated, as it does not correspond to a Hermitian operator. A widely accepted approach involves the two-point energy measurement scheme, where the energy is measured at the beginning and end of a dynamical process [65]. If the Hamiltonian changes in time due to external driving, the system evolves unitarily, and the average work performed,

$$\langle W \rangle = \sum_{m,n} (E_m^{(f)} - E_n^{(i)}) P_{mn} p_n.$$

Here, p_n denotes the initial probability of the system occupying the n-th eigenstate, while P_{mn} represents the likelihood of transitioning to the m-th eigenstate in the final state.

1.7.5 Quantum friction

Quantum friction refers to the generation of non-adiabatic excitations when a quantum system is driven rapidly. In the quantum regime, unlike in classical systems, such friction manifests as coherence and entropy production [63]. These effects are significant in quantum heat engines and other cyclic processes, as they reduce efficiency and increase entropy production. Minimising quantum friction through shortcut-to-adiabaticity techniques or optimal control is an active area of research.

1.7.6 Thermodynamic processes

Quantum analogues of classical thermodynamic processes can be realised under appropriate conditions:

- **Adiabatic process:** Here heat is exchange is absent. In the quantum setting, this corresponds to adiabatic evolution, assuming the system follows the instantaneous eigenstate of the Hamiltonian throughout a slow evolution without encountering energy level crossings.
- **Isothermal process:** The system interacts thermally with a heat reservoir maintained at a fixed temperature. Heat exchange and work are both involved, and the system evolves towards a thermal equilibrium state.
- **Isochoric process:** In this process, a control parameter such as volume remains fixed. No work is done; changes in internal energy occur only owing to heat exchange with the environment.
- **Isobaric process:** Although less straightforward to define in quantum mechanics, analogues can be constructed by fixing generalised force variables such as external fields, with appropriate conjugate observables.

These processes can be engineered in quantum platforms, such as cold atoms, superconducting qubits, or trapped ion systems, through precise manipulation of control parameters and reservoir coupling [63].

1.7.7 Irreversibility and entropy production

As discussed previously, entropy in quantum systems is quantified by the von Neumann entropy:

$$S(\rho) = -\mathrm{Tr}(\rho \log \rho).$$

During irreversible processes—such as sudden quenches or non-adiabatic driving—entropy is produced, and the system deviates from equilibrium. The total entropy change, including that of the environment, satisfies the second law of thermodynamics:

$$\Delta S_{\mathrm{tot}} \geq 0.$$

In modern formulations, entropy production may also include contributions from quantum coherence and correlations, leading to generalised second laws involving quantum information-theoretic measures [65].

A deeper understanding of irreversibility in quantum systems is obtained by analysing the difference between the evolved non-equilibrium state $\rho(t)$ and the corresponding equilibrium (Gibbs) state $\rho_{\mathrm{eq}} = e^{-\beta H}/Z$. This is formalised using the Kullback–Leibler (KL) divergence, also referred to as the quantum relative entropy:

$$D(\rho(t)\|\rho_{\mathrm{eq}}) = \mathrm{Tr}\left[\rho(t)\log\rho(t) - \rho(t)\log\rho_{\mathrm{eq}}\right].$$

This quantity is always non-negative and vanishes if and only if $\rho(t) = \rho_{\mathrm{eq}}$. It quantifies the degree of thermodynamic irreversibility by indicating the system's deviation from

equilibrium. In many formulations, the entropy production Σ is directly identified with the KL divergence:

$$\Sigma = D(\rho(t)\|\rho_{\text{eq}}),$$

providing a strong connection between statistical irreversibility and information loss. This framework also generalises to situations involving feedback, measurements, and quantum coherence [65]. More details about how KL divergence and its relationship with irreversibility can be seen in Chapter 5.

1.7.8 Applications: quantum heat engines and thermal control

The principles of quantum thermodynamics are applied in the development and evaluation of quantum heat engines, refrigerators, and energy storage devices such as quantum batteries. These devices utilise quantum resources, such as coherence and entanglement, to potentially outperform classical counterparts [66, 67]. Important examples include quantum Otto and Carnot engines employing two-level systems or harmonic oscillators as working substances.

Additionally, quantum thermodynamic effects are crucial in the operation of quantum information processors. For instance, *thermal throttling*—the dynamic regulation of heat in quantum circuits—ensures stable operation and protects coherence. Likewise, *quantum friction* becomes a limiting factor in high-speed gate operations and must be mitigated to achieve optimal performance in next-generation quantum technologies.

We can now provide a brief overview of the various heat engine models that are widely considered by researchers.

1.7.9 Quantum heat engine models

Quantum heat engines (QHEs) are quantum analogues of classical thermal machines, operating on similar thermodynamic cycles but governed by quantum mechanical laws. Several theoretical models of QHEs have been proposed, each exploring different working substances, operational cycles, and coupling mechanisms.

Three-level maser engine: One of the earliest QHE models is the three-level maser proposed by Scovil and Schulz-DuBois [68], which can be regarded as a quantum analogue of the classical Carnot engine. It operates by facilitating population inversion between discrete energy levels, extracting work via coherent radiation.

Quantum Otto engine: The quantum Otto engine is a popular and widely studied model [66, 69], where the working medium undergoes a four-stroke cycle analogous to the classical Otto engine. The system typically consists of harmonic oscillators or spin systems, with strokes including isentropic (unitary) and isochoric (thermalising) transformations.

Quantum Stirling and Carnot engines: Extensions of classical Stirling and Carnot engines into the quantum domain have also been investigated [70]. These models provide insights into maximum efficiency conditions, coherence effects, and entropy generation in idealised quantum systems.

Each of these engine types exhibits unique quantum features, such as coherence, entanglement, and energy quantisation, and studying their behaviours under various simulation conditions helps us to expand our understanding of the interplay between quantum mechanics and thermodynamics [62, 63].

Now, let us have a look at the efficiency of these quantum heat engines.

1.7.10 Quantum heat engines: Efficiency

A heat engine's efficiency is determined by the proportion of net work produced relative to the heat absorbed from the high-temperature reservoir. In the classical domain, the

maximum theoretical efficiency is given by the Carnot efficiency,

$$\eta_{\text{Carnot}} = 1 - \frac{T_L}{T_H}.$$

Where T_H and T_L are the temperatures of the hot (source) and cold (sink) reservoirs, respectively. This limit is universal for all engines operating between two thermal baths, under the assumptions of quasistatic and reversible operation.

In the quantum regime, the Carnot efficiency serves as the upper bound, whereas the characteristics of quantum working substances lead to distinct thermodynamic behaviour. For instance, discrete energy levels, quantum coherence, and entanglement can affect the engine performance. Particularly, for engines operating in finite time or involving rapid driving, the efficiency tends to be lower than the Carnot limit.

For quantum Otto engines, the efficiency under ideal conditions (i.e., perfect adiabatic strokes and thermalisation) is given by:

$$\eta_{\text{Otto}} = 1 - \frac{\omega_L}{\omega_H}.$$

Where ω_H and ω_L denote the system frequencies during the hot and cold isentropic strokes, respectively. This expression reflects the role of energy level spacing, which is modulated externally.

Quantum friction and irreversibility: Realistic quantum engines deviate from ideal conditions owing to non-adiabatic transitions and finite-time operations. This leads to unwanted excitations and entropy production, thereby reducing the actual work output, a phenomenon known as *quantum friction* [63, 65].

The reduction in performance can be quantitatively described by introducing the concept of irreversible work:

$$W_{\text{ir}} = \langle W \rangle - \Delta F.$$

Where ΔF represents the difference in free energy between the initial and final thermal states. The irreversible entropy production Σ is frequently expressed in terms of the quantum relative entropy (or Kullback—Leibler divergence) between the actual state ρ and the instantaneous thermal equilibrium state ρ_{eq} as:

$$\Sigma = S(\rho||\rho_{\text{eq}}).$$

Actual Efficiency: Taking losses into account, the efficiency becomes:

$$\eta_{\text{actual}} = \frac{W_{\text{out}}}{Q_H} = \eta_{\text{ideal}} - \delta\eta.$$

Where $\delta\eta$ represents the correction due to quantum friction and non-ideal thermalisation. Optimising the driving protocols using shortcuts to adiabaticity (STA) or counter-adiabatic driving can help suppress quantum friction and enhance efficiency [62].

Thus, the efficiency of quantum heat engines is constrained not only by thermodynamic laws but also by the nature of quantum dynamics, and achieving high efficiency requires carefully balancing speed, control, and coherence.

1.8 Unitary dynamics of quantum systems

In quantum mechanics, the evolution of an isolated system is governed by *unitary dynamics*, a direct consequence of the linearity of the theory and the requirement that probabilities remain conserved over time. This framework provides a deterministic and reversible evolution of quantum states in Hilbert space and is central to understanding quantum processes in closed systems. This section discusses the theoretical structure of unitary evolution, how quantum states and observables evolve, and which physical quantities remain conserved as a result [71, 72].

1.8.1 Evolution of quantum states: The Schrödinger picture

The evolution of a closed quantum system is governed by the time-dependent Schrödinger equation:

$$i\hbar\frac{d}{dt}|\psi(t)\rangle = \hat{H}(t)|\psi(t)\rangle, \tag{1.14}$$

where $|\psi(t)\rangle$ is the state vector at time t, and $\hat{H}(t)$ is the Hamiltonian operator, which may in general be time-dependent.

We introduce the *time-evolution operator* $\hat{U}(t,t_0)$ to determine the state at a later time t, satisfying

$$|\psi(t)\rangle = \hat{U}(t,t_0)|\psi(t_0)\rangle, \tag{1.15}$$

with the initial condition $\hat{U}(t_0,t_0) = \mathbf{I}$. This operator must be unitary, i.e.,

$$\hat{U}^\dagger(t,t_0)\hat{U}(t,t_0) = \mathbf{I}, \tag{1.16}$$

to ensure that the norm of the state—and hence total probability—is preserved. When the Hamiltonian is time-independent, the evolution operator takes the form

$$\hat{U}(t,t_0) = e^{-i\hat{H}(t-t_0)/\hbar}. \tag{1.17}$$

For time-dependent Hamiltonians, one must account for the noncommutativity of $\hat{H}(t)$ at different times. The general solution is written using a *time-ordered exponential*:

$$\hat{U}(t,t_0) = \exp\left(-\frac{i}{\hbar}\int_{t_0}^{t}\hat{H}(s)\,ds\right), \tag{1.18}$$

This process gives the full time evolution of the quantum state within the Schrödinger picture.

1.8.2 Evolution of observables: The Heisenberg picture and conservation laws

An alternative description of quantum dynamics is given by the *Heisenberg picture*, where the states remain constant while the operators evolve over time. The time evolution of an operator $\hat{O}$ is expressed as:

$$\hat{O}_H(t) = \hat{U}^\dagger(t,t_0)\,\hat{O}_S\hat{U}(t,t_0), \tag{1.19}$$

where $\hat{O}_S$ is the operator in the Schrödinger picture, and $\hat{O}_H(t)$ is its Heisenberg-evolved counterpart. This transformation preserves the expectation value:

$$\langle\psi(t)|\hat{O}_S|\psi(t)\rangle = \langle\psi(t_0)|\hat{O}_H(t)|\psi(t_0)\rangle. \tag{1.20}$$

Differentiating the Heisenberg operator with respect to time yields the *Heisenberg equation of motion*:

$$\frac{d}{dt}\hat{O}_H(t) = \frac{i}{\hbar}[\hat{H}_H(t),\hat{O}_H(t)] + \left(\frac{\partial\hat{O}_S}{\partial t}\right)_H, \tag{1.21}$$

which is the quantum analogue of classical Hamilton's equations. The last term accounts for any explicit time dependence of the operator.

Conservation laws One of the key implications of unitary evolution is the conservation of certain physical quantities. An observable $\hat{Q}$ is said to be *conserved* if its expectation value remains constant in time:

$$\frac{d}{dt}\langle\hat{Q}_H(t)\rangle = 0. \tag{1.22}$$

From the Heisenberg equation, this condition holds if

$$[\hat{H}, \hat{Q}] = 0 \quad \text{and} \quad \frac{\partial \hat{Q}}{\partial t} = 0. \tag{1.23}$$

That is, a time-independent operator that *commutes with the Hamiltonian* is a constant of motion. This links conservation laws in quantum mechanics to symmetries of the system via *Noether's theorem*. For example:

- Translational symmetry $\Rightarrow$ conserves momentum
- Rotational symmetry $\Rightarrow$ conserves angular momentum
- Time-translation symmetry $\Rightarrow$ conserves energy

These symmetries are embedded in the structure of the Hamiltonian and are preserved under unitary evolution.

Now, let us look at some of the most important observables in quantum many-body systems, which are relevant to our work.

1.9 Entropy

Around 60 years ago, Claude Shannon laid the theoretical groundwork for Information Theory [73]. This theory primarily focuses on evaluating the efficiency of information transfer by using complexity measures, such as entropy, within the context of the signal space communication framework. Shannon's *source coding theorem* was a pioneering concept in lossless data compression, where he defined a limit on how much a source's output can be compressed without losing information, quantified by the entropy of the source. Prior to Shannon's groundbreaking contributions, entropy was introduced in thermodynamics and statistical mechanics by Clausius and Boltzmann, respectively. In

these fields, entropy was used as a measure to characterize the properties of physical systems.

Shannon's entropy formulation was based on discrete probability theory and built upon the idea that 'information gained from a system with high uncertainty holds significant value.' He introduced two central concepts: (1) entropy, which measures the information content of a system's state, and (2) mutual entropy, which quantifies the information transmitted from an initial system to a final system through a channel. This theory of entropy, in line with the development of probability theory, provided a mathematical foundation for classical information theory. Key components of this foundation include Kullback–Leibler's relative entropy [74] and the mutual entropy formulation by Gelfand–Kolmogorov–Yaglom [75, 76], applied within continuous probability spaces.

The exploration of entropy within quantum systems commenced in 1932 with von Neumann [77, 78], and Umegaki [78] introduced quantum relative entropy. This concept was further extended to general quantum systems by Araki [79, 80], Uhlmann [81], and Donald [82]. Notably, von Neumann [77] defined quantum entropy for a density operator approximately two decades before the development of Shannon entropy.

1.9.1 Von Neumann entropy

In physics, the von Neumann entropy [83], named after John von Neumann, represents an extension of the classical statistical mechanics concept of Gibbs entropy into the domain of quantum statistical mechanics. We partition our extensive system into two components, denoted as Q and its complement, $\tilde{Q}$. The composite Hilbert space H_S of the entire system is the tensor product of the local Hilbert spaces H_Q and $H_{\tilde{Q}}$. The computation of entanglement entropy involves examining the reduced density matrix of the subsystem Q, denoted as ρ_Q, and subsequently evaluating the von Neumann entropy using the formula:

$$\mathscr{S}_Q = -\mathrm{tr}(\rho_Q \log(\rho_Q))$$

A nonzero value for $\mathscr{S}_Q$ indicates entanglement between the two subsystems. The magnitude of the entanglement entropy reflects the extent of entanglement existing between these two subsystems. We will revisit von Neumann entropy several times in the upcoming chapters.

1.9.2 Topological entanglement entropy

The topological entanglement entropy (TEE), denoted as $\mathscr{S}_{topo}$, serves as a universal measure characterising the quantum entanglement in the ground state of a two-dimensional topologically ordered medium with a mass gap [84, 85]. In the context of bipartite entanglement entropy (EE), which quantifies the degree of entanglement between partitions of a system, it has been observed that EE follows an "area law." This implies that the entanglement entropy is proportional to the boundary between the two partitions. Kitaev and Preskill [84] as well as Levin and Wen [85] independently demonstrated, in their respective works, that beyond the area-dependent term, there exists a component of the entanglement entropy solely dependent on the topology of the boundary curve. This component is termed the topological entanglement entropy (TEE).

The definition of TEE involves three partitions of the system denoted as A, B, and C, with the remaining part labelled as D as seen in the Fig 1.8. The entanglement entropies of the subsystems A, B, C, $A\cup B$, $B\cup C$, $A\cup C$, and $A\cup B\cup C$ are represented by $\mathscr{S}_A$, $\mathscr{S}_B$, $\mathscr{S}_C$, $\mathscr{S}_{A\cup B}$, $\mathscr{S}_{B\cup C}$, $\mathscr{S}_{A\cup C}$, and $\mathscr{S}_{A\cup B\cup C}$, respectively.

The formula for TEE ($\mathscr{S}_{topo}$) is expressed as:

$$\mathscr{S}_{topo} = \mathscr{S}_A + \mathscr{S}_B + \mathscr{S}_C - \mathscr{S}_{A\cup B} - \mathscr{S}_{B\cup C} - \mathscr{S}_{A\cup C} + \mathscr{S}_{A\cup B\cup C}. \tag{1.24}$$

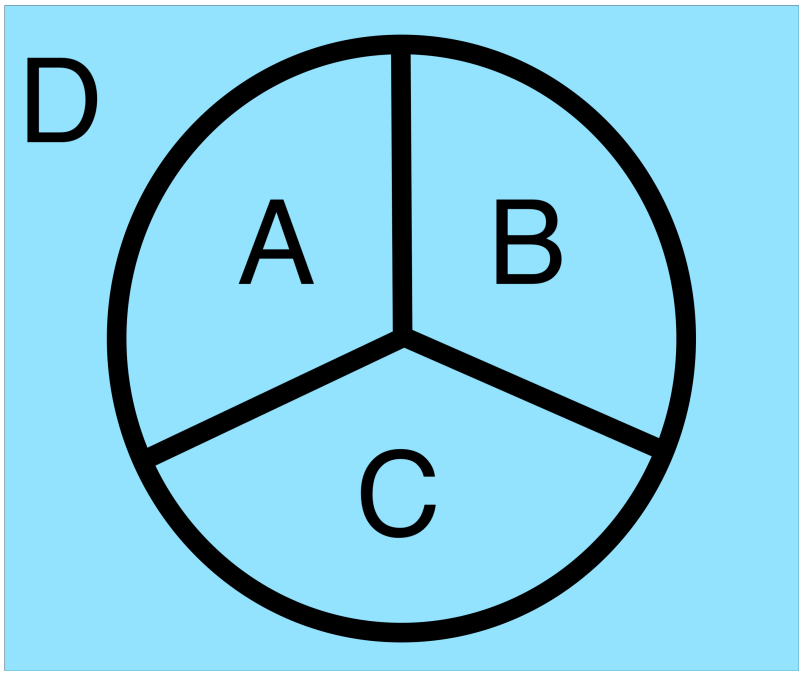

Fig. 1.8 The two-dimensional lattice is divided into four regions A, B, C, and D. Care is given to avoid sharp features as much as possible

For a large system, $\mathscr{S}_{topo}$ is defined to remain invariant under smooth deformations of the Hamiltonian and only undergo changes when encountering a quantum critical point. In chapters 3 and 4. We will revisit TEE in the upcoming chapters.

1.9.3 Kullback–Leilbler Divergence class

The Kullback–Leibler Divergence, also known as relative entropy, encompasses a wider concept of divergence. It quantifies the degree of deviation between a given probability distribution and an expected reference probability distribution. The Kullback–Leibler divergence finds practical applications in various real-time scenarios. The Kullback–Leibler Divergence Class, or relative entropy, represents a more comprehensive form of divergence. It involves the evaluation of how one probability distribution differs from another expected probability distribution. It measures the “distance" between these two distributions, indicating the amount of information lost when one distribution is employed

to approximate the other. In information theory, entropy is used to measure the uncertainty linked to a random variable. Simply put, it represents the average amount of 'surprise' you might expect when learning the outcome of the variable. The entropy for a discrete random variable x with a probability mass function $P(x)$, can expressed as:

$$S_p = -\sum P(x) log(P(x)) \tag{1.25}$$

Consider another probability distribution of the same random variable x, $Q(x)$. Then the relative entropy between P and Q is defined as follows.

$$D_{KL}(P||Q) = \sum P(x) \log(\frac{P(x)}{Q(x)}) \tag{1.26}$$

Here, the sum runs over all possible outcomes. P is the original or initial distribution, and Q is the estimated final distribution. Relative entropy is a positive quantity, and it is not symmetric. Meaning $D_{KL}(P||Q) \neq D_{KL}(Q||P)$. In quantum many-body theory, we often use the relative entropy to quantify the relative distance between two quantum states. When the two distributions considered are the initial and final thermal density matrices, followed by a thermodynamic process, we call the resulting density matrix the irreversible entropy between the two processes. This quantifies the amount of irreversible work done by the system.

In the next section, we will see what inspired this thesis and how it is relevant to the field.

1.10 Motivation

Magnetic skyrmions are important to spintronics and quantum computing fields alike. Each coming day, various applications of skyrmions are being uncovered. Fert *et al.* (2013) [54] demonstrated that electric currents can be utilised to manipulate skyrmions.

This finding marks a notable advancement in the potential application of skyrmions in spintronic devices. In a recent study by Wang and colleagues (2022) [86], the researchers showcase the capability of skyrmions to function as reliable sources for true random number generation, particularly for applications in probabilistic computing. These are only a few of the potential applications of skyrmions, with a focus on the quantum mechanical study of nano-scale skyrmions, which can significantly contribute to this field. The topological nature of materials imparts them with previously undiscovered characteristics, making this thesis a noteworthy contribution to the field.

Our main goals include:

1. Investigating various materials and methods to achieve quantum magnetic skyrmions through numerical calculations.

2. Theoretical exploration of different approaches to quantify the topological order in skyrmions.

3. Examination of the physical properties arising from topological protection.

4. Identification of potential applications for magnetic skyrmions.

All the objectives have been successfully achieved and are comprehensively documented in this thesis.

1.11 Outline of the thesis

The remainder of the thesis is organised into four primary chapters and a concluding summary chapter. In Chapter 2, we introduce a novel lattice model for simulating skyrmions. This involves a review of existing quantum mechanical studies, an examination of their limitations, and an exploration of the enhancements provided by our model. We employ local magnetisation and structure factors to detect spin textures, while scalar chirality is

utilised to identify topological order and construct a phase diagram. The energy levels demonstrate the stability of topological order in the lower energy states. Additionally, we investigate any indications of dynamical quantum phase transitions following specific quenches.

Moving on to Chapter 3, we look into a quantum model for skyrmions and characterise it using standard observables. A novel topological quantifier, known as topological entropy, is introduced to discern topological order. This quantifier proves to be effective in identifying phase boundaries and indicates increased stability of skyrmions with higher next-nearest-neighbour interaction strength.

Chapter 4 focuses on exploring the dynamical behaviour of significant quantities related to magnetic systems and topologically ordered systems. We investigate the impact of dynamical quantum phase transitions on entropy production.

In Chapter 5, we propose an application for skyrmions by exploring a theoretical model of a plasmonic skyrmion heat engine. Here we mainly employ quantum thermodynamics, emphasising on relative entropy. We investigate how topological order influences various aspects of the system, including the amount of work lost during an Otto cycle and the efficiency of the engine. Additionally, the physical system on which our engine is modelled has a flexible system size, which can be controlled to extract desired output power.

Finally, in the concluding chapter, we provide a comprehensive summary of all relevant information for a quick overview. Additionally, each chapter includes appendices containing supplementary or equally important information related to the respective chapters.